PHYSICAL REVIEW VOLUME 92, NUMBER 5 DECEMBER 1, 1953

Magnetization in Nickel Ferrite-Aluminates and Nickel Ferrite-Gallates*†

LOUIS R. MAXWELL AND STANLEY J. PICKART
Naval Ordnance Laboratory, White Oak, Maryland

(Received August 25, 1953)

Trivalent aluminum and trivalent gallium have been substituted for trivalent iron in nickel ferrite $NiO \cdot Fe_2O_3$ to give the systems $NiO \cdot Fe_{2-t}Al_tO_3$ and $NiO \cdot Fe_{2-t}Ga_tO_3$, respectively, where t goes from 0 to 2. The materials, annealed and prepared in a powdered form, were homogeneous with the length of the edge of the unit cell decreasing linearly from 8.332A to 8.043A and 8.247A, for the aluminum and gallium substitution, respectively, as t varies from 0 to 2. In the case of the aluminum substitution, thermomagnetic curves were obtained of the types classified by Néel as Q; M_1, M_2, or P; and type R. The saturation magnetization extrapolated to 0°K (μ_0) for the nickel ferrite-aluminates decreases linearly with increase in t approaching zero in the region of $t=0.63$; for further increase in t, μ_0 increases to a maximum at about $t=1.0$ beyond which it decreases again to 0 at $t=2$. The increase in μ_0 is interpreted as an indication of a reversal in the direction of the resultant magnetization due to predominance of the magnetization of the ions on the A sites over those on the B sites. For the gallium substitution, the thermomagnetic curves follow the more conventional Q type with the appearance of the R-type curves for values of t from 0.63 to 1.5. As contrasted to the aluminates, the gallates show an increase in μ_0 with t, with a maximum developing in approximately the same region where the aluminates showed the crossover from B dominance to A dominance. The Curie temperatures decrease near-linearly with increase in t; the points for the aluminates and the gallates are so close together that they can be represented by one smooth curve. From an application of the Néel theory, it is indicated that the BB interaction is negative, both for the aluminates and the gallates, at least for values of t in the region 0.63 to 1.00.

I. INTRODUCTION

An insight into the magnetic behavior of the ferrites can be gained by performing certain substitutions for the ferric ion. Michel and Pouillard[1] substituted Al^{3+} for Fe^{3+} in Fe_3O_4, and they found that both the Curie temperature and size of the unit cell decreased linearly with the amount of aluminum added until a point was reached where approximately one ion out of seven Fe^{3+} was replaced by one Al^{3+}; beyond this point, both the Curie temperature and size of unit cell remained constant. They concluded from this work that only a limited amount of aluminum can be held in solid solution with Fe_3O_4.

Thermomagnetic investigations of promoted, unreduced iron oxide catalysts were carried out by Maxwell, Smart, and Brunauer[2] on Fe_3O_4 containing up to about 35 mole percent of Al_2O_3. The Curie temperature remained constant with a reduction in the intensity of magnetization roughly proportional to the volume occupied by the Fe_3O_4 which indicated that the Al_2O_3 existed either as a separate phase or possibly in combination with FeO to form a ferrous aluminate.

Guillaud and Michel[3] have found a linear decrease in the saturation magnetic moment for magnetite with aluminum substituted until there was approximately 0.20 of an aluminum ion per molecule, presumably in solid solution. Although the authors state that their data is in agreement with the Néel theory,[4] the way in which this agreement is established is not clear because of the lack of sufficient information as to the distribution of the magnetic ions in the lattice.

The replacement of trivalent iron in Fe_3O_4 is complicated by the fact that the iron ion can go from the ferrous to ferric state rather easily by a simple transfer of an electron. It, therefore, is desirable to perform substitution experiments with a material having a more stable divalent ion.

Jones and Roberts[5] have carried out a series of substitutions of Fe^{3+} for Al^{3+} in magnesium ferrite ($MgO \cdot Fe_2O_3$). From thermomagnetic measurements they found that the saturation magnetization, at low temperature, decreased as Al^{3+} replaced Fe^{3+}, with a certain irregularity which they ascribed to heat treatment, until $MgAlFeO_4$ was reached which had a moment of about 0.3 Bohr magneton per molecule. The end points of this substitution series were investigated by neutron diffraction by Bacon and Roberts[6] who showed them to be

$$[Mg_{0.1}Fe_{0.9}]_A[Mg_{0.9}Fe_{1.1}]_BO_4$$

and

$$[Mg_{0.53}Fe_{0.47}]_A[Mg_{0.47}AlFe_{0.53}]_BO_4,$$

respectively, in agreement with the magnetic measurements and with earlier x-ray investigations by Greenwald[7] and Bertaut.[8]

Since the Al^{3+} ions apparently prefer to move into the B sites,[9] it is of interest to study such a substitution when the divalent ion has a magnetic moment as in the case of nickel ferrite ($NiO \cdot Fe_2O_3$). Because the nickel ferrite is inverted, we have a situation where

---

* This work was supported in part by the U. S. Office of Naval Research.

† Presented in part at the March Meeting (1953) of the American Physical Society [Phys. Rev. **91**, 206 (1953)].

[1] A. Michel and E. Pouillard, Compt. rend. **227**, 194 (1948).

[2] Maxwell, Smart, and Brunauer, J. Chem. Phys. **19**, 303 (1951).

[3] C. Guillaud and A. Michel, J. phys. et radium **12**, 65 (1951).

[4] L. Néel, Ann. phys. **3**, 137 (1948).

[5] G. O. Jones and F. F. Roberts, Proc. Phys. Soc. (London) **B65**, 390 (1952).

[6] G. E. Bacon and F. F. Roberts, Acta. Cryst. **6**, 57 (1953).

[7] Selma Greenwald, Naval Ordnance Laboratory Memorandum 10504, 1950 (unpublished).

[8] E. F. Bertaut, J. phys. et radium **12**, 252 (1951).

[9] E. J. W. Verwey and E. L. Heilmann, J. Chem. Phys. **15**, 174 (1947).

we expect that the aluminum ions will deplete the total magnetization arising from the ions in the *B* sites without a strong reduction in the intensity of magnetization of the ions in the *A* sites. As a result, a point should be reached where the intensity of magnetization of the magnetic ions on the *B* and *A* sites should be nearly equal and opposite so that the resultant magnetization of the material should approach zero—or similar to the antiferromagnetic state.

Trivalent gallium[10] has certain preferential tendencies for the tetrahedral interstices. It is listed by Verwey and Heilman[9] as one of the exceptions to a general rule laid down by them for the position of the trivalent and quadrivalent ions in accordance with the electrostatic requirements for minimum Coulomb energy. We will include in this paper the substitution of Ga^{3+} for Fe^{3+} in the nickel ferrite. The movement of Ga^{3+} to the tetrahedral interstices should mean an initial increase in the resultant magnetization. We, therefore, expect that in this substitution we would not reach a point where the magnetization from the *B* and *A* sites would be equal and opposite. An important point is the way in which Fe^{3+} and Ga^{3+} compete for the *A* sites.

II. PROCEDURE AND EXPERIMENTAL ARRANGEMENT

(a) Preparation of Materials

The materials used in this investigation are called the nickel ferrite-aluminates and nickel ferrite-gallates, defined by $NiO \cdot Fe_{2-t}Al_tO_3$ and $NiO \cdot Fe_{2-t}Ga_tO_3$, respectively. The parameter t was varied in steps ranging from 0 to 2, which covered the entire range from nickel ferrite to nickel aluminate ($NiO \cdot Al_2O_3$) and nickel gallate ($NiO \cdot Ga_2O_3$).

The substances were prepared following the procedures outlined by Harvey *et al.*,[11] using the oxides as the starting materials. The components were first mixed by the use of a ball mill containing a water slurry of the oxides. After the water was removed and the material ground in a mortar and pestle, it was heated to 1000°C for two hours, cooled, reworked, and heated a second time to 1000°C after the material has been passed through a 200-mesh sieve. The final heating carried the material up to a temperature of 1410°C for one hour. The cooling rate from this temperature was controlled, and in most instances was lowered at the rate of approximately 1° per minute. All of the heat treatments were carried out in air. It was found that platinum boats proved to be more suitable as containers for these materials than the usual oxide type boat.

(b) Intense Magnetic Field Solenoid

A high-current solenoid was constructed for this work to produce a field having a maximum strength of 8000 oersteds without using ferromagnetic materials. A diagrammatic sketch of the solenoid is shown in Fig. 1. The windings are 0.025-in. thick copper ribbons 0.875 in. in width wound concentrically with insulating glass cloth separating adjacent turns. The cooling was accomplished by inserting between each coil a circular water layer as illustrated in Fig. 1. An efficient labyrinth was devised so that the incoming cool water proceeded directly, after a few revolutions, to the inner diameter of the coil and then back out again, like a noninductive winding, to the exhaust without encountering any dead air pockets. The solenoid operates at a maximum current of 100 amperes at 300 volts.

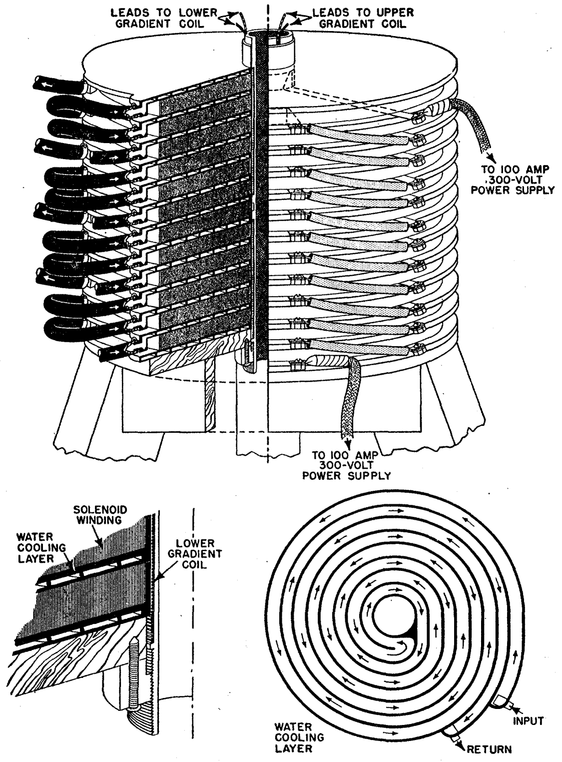

FIG. 1. Sketch of air core solenoid for producing intense magnetic fields. Dimensions of solenoid windings: length = 32.0 cm, inside diameter = 6.25 cm, outside diameter = 43.2 cm.

(c) Gradient Coils

A pair of opposing solenoid coils were mounted inside the large solenoid in such a way as to deliver at the center of the solenoid system a variable magnetic field gradient that is uniform over an appreciable volume. The nature of this gradient is illustrated in Fig. 2. It is seen that the resultant gradient is constant for a distance of 2 cm.

(d) The Method

We measure the intensity of magnetization of the specimen as a function of the applied field and the temperature of the material. This is accomplished by a

---

[10] F. Machatschki, Z. Krist. **82**, 348 (1932).

[11] Harvey, Hegyi, and Leverenz, R.C.A. Rev. **12**, 344 (1950).

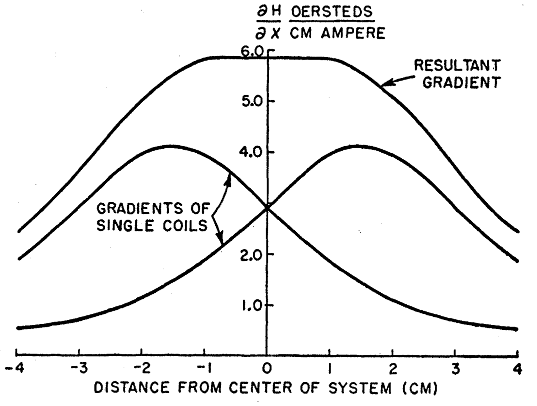

FIG. 2. Relationship between magnetic field gradient, produced by gradient coils (solenoid), as a function of distance. Distance between adjacent ends of coils = 3 cm; radius = 3 cm.

force method, using the following equation:

$$F = IV\partial H/\partial x, \tag{1}$$

where F is the force upon the specimen having an intensity of magnetization I, a volume V, in the presence of a magnetic field gradient of $\partial H/\partial x$.

We have, by this method, control of the force on the sample through the independent variation of the magnetic field and the magnetic-field gradient.

The way in which the force is measured is illustrated diagrammatically by Fig. 3. The specimen is suspended by a fine wire from a lever arrangement coupled to the winding of a Schaevitz differential transformer whose magnetic core is held in a fixed position. The output from this transformer varies linearly with the displacement of the winding with respect to the core at a usual sensitivity of 0.025 volt per 0.001-in. displacement. A recorder measures the signal output of the transformer. The force acting on the sample produces a small displacement of the transformer winding which appears as a deflection on the recorder. Although this is a deflection method, it is also, in effect, a null method because the displacements of the sample are so small—0.010-in. maximum for full-scale deflection—that over the region in which the specimen moves both the magnetic field and the gradient remain constant.

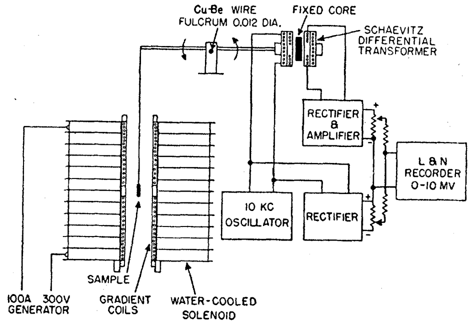

FIG. 3. Diagrammatic sketch of apparatus for measuring intrinsic magnetic moments.

The specimens were in a powdered form occupying a volume of 10 mm in length with a diameter of 1 mm. A piece of pure nickel (assumed to have a moment at 20°C of 0.57 Bohr magneton per atom)[12] of approximately the same size was used for calibration giving directly the deflections of the recorder in units of Bohr magnetons per molecule. The necessary furnaces and equipment for cooling the specimen are not shown in Fig. 3.

III. RESULTS

(a) Structure of Materials

Powder x-ray diffraction photographs showed, in all cases, a spinel structure whose length of edge of unit cell (a_0) varied in a linear fashion as shown by Fig. 4. The end points, corresponding to the nickel ferrite and nickel aluminate, are in essential agreement with previous values.[9] The size of the unit cell for all the intermediate points varied in a systematic manner. In no cases were there lines present due to the initial oxides that were used as starting materials.

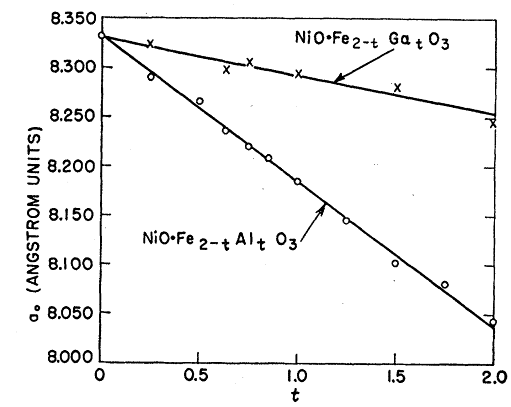

FIG. 4. Variation of unit cell size (a_0) with composition for $NiO \cdot Fe_{2-t}Al_tO_3$ and $NiO \cdot Fe_{2-t}Ga_tO_3$.

(b) Thermal Magnetization Data

The saturation magnetization (μ), sometimes called technical magnetization, was measured as a function of temperature, from liquid nitrogen temperature through the Curie temperature and beyond far enough to find any ferrimagnetism of the type predicted by Néel's N-type curve. The results are shown in Fig. 5 in a normalized form for both the aluminates and gallates; no N types were found in either series.

The way in which the saturation magnetization, extrapolated to absolute zero (μ_0), varies with the composition is shown in Fig. 6. Data are given for both quenched and annealed samples for both the aluminates and the gallates. The information on the aluminates has been expanded into three dimensions by a model

---

[12] R. M. Bozorth, *Ferromagnetism* (D. Van Nostrand Company, Inc., New York, 1951), p. 867.

illustrated in Fig. 7, which gives the relationship between the intensity of magnetization with respect to temperature and composition. The contour lines representing constant magnetization are illustrated for both positive and negative values.

The variation of Curie temperature with composition is illustrated in Fig. 8. The results for both of the systems studied can be represented by a single curve that departs slightly from linearity.

IV. DISCUSSION

The x-ray studies showed that the materials were in all cases homogeneous having the spinel structure. In the case of the aluminum substitutions the linear decrease in the size of the unit cell was expected since the trivalent radius of aluminum is 0.57A as compared to 0.67A the radius of Fe^{3+} as given by Goldschmidt. For the gallium substitution there was only a slight decrease with increasing amounts of gallium. This is explained by the fact that the radius of Ga^{3+} is very close to that of Fe^{3+}.

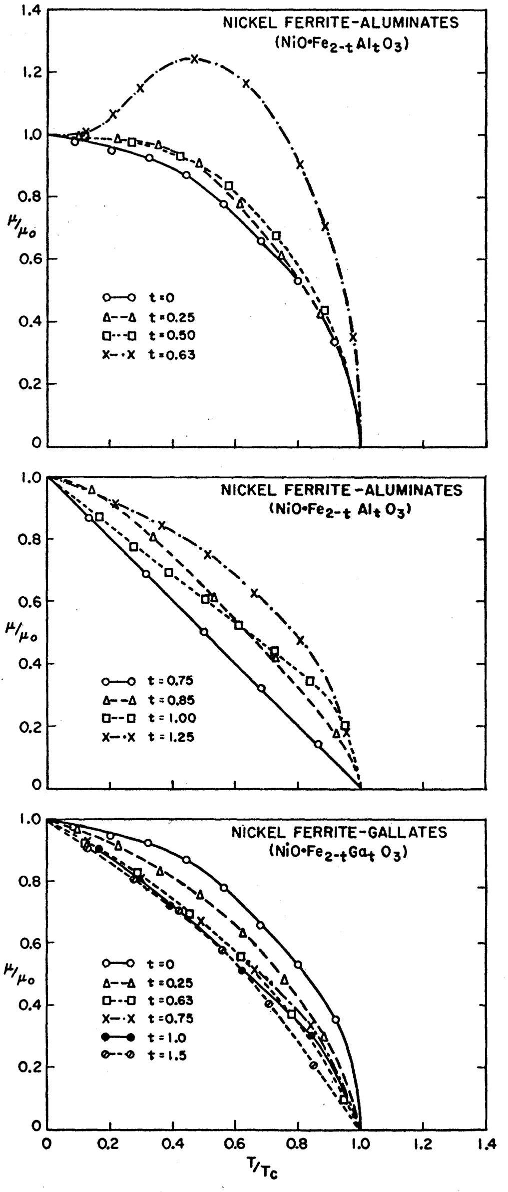

FIG. 5. Normalized thermomagnetization curves (annealed at 1°/min) for $NiO\cdot Fe_{2-t}Al_tO_3$ and $NiO\cdot Fe_{2-t}Ga_tO_3$.

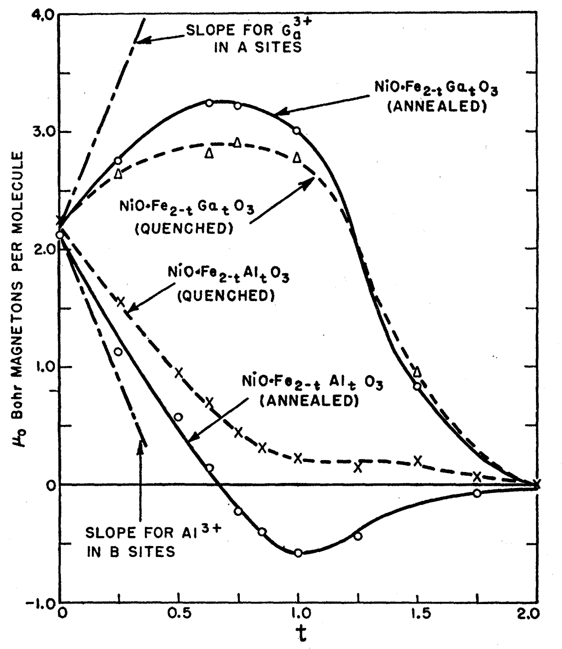

FIG. 6. Variation of μ_0 with composition for $NiO\cdot Fe_{2-t}Al_tO_3$ and $NiO\cdot Fe_{2-t}Ga_tO_3$ annealed at 1°/min, quenching carried out from 1410°C.

The thermomagnetization curves obtained for nickel ferrite-aluminate, as illustrated in Fig. 5, can be considered in terms of the Néel theory.[4] We have for the magnetizations M_a and M_b of the A and B lattice sites, respectively, for N magnetic ions (only one kind):

$$\begin{aligned} M_a &= \lambda N g\beta S B_S(g\beta S H_a/kT), \\ M_b &= \mu N g\beta S B_S(g\beta S H_b/kT), \end{aligned} \tag{2}$$

where λ and μ are the fraction of magnetic ions on the A and B sites, respectively; H_a and H_b are the effective fields acting on the magnetic ions in the A and B sites, respectively, which are expressed in terms of the molecular field coefficients (γ's) as

$$\begin{aligned} \mathbf{H}_a &= \mathbf{H}_0 + \gamma_{aa}\mathbf{M}_a - \gamma_{ab}\mathbf{M}_b, \\ \mathbf{H}_b &= \mathbf{H}_0 - \gamma_{ab}\mathbf{M}_a + \gamma_{bb}\mathbf{M}_b, \end{aligned} \tag{3}$$

where γ_{ij} is the Weiss molecular field coefficient for the interaction between the ions on the ith and jth sites. $B_S(\ )$ is the Brillouin function.

In the ferrimagnetic case we obtain the spontaneous magnetization ($H_0=0$) from Eqs. (2) and (3) in terms of the specific magnetization $\mathcal{Y}_a$ and $\mathcal{Y}_b$, given in terms

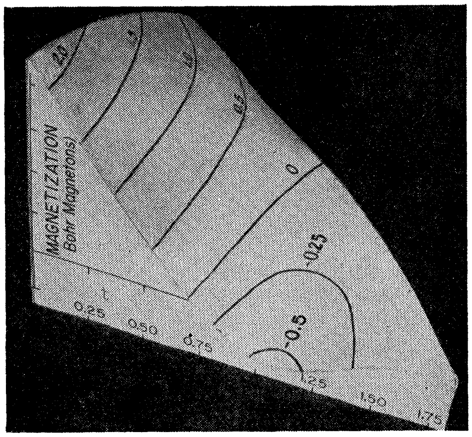

FIG. 7. Photograph of three dimensional model of the system nickel ferrite-aluminate. Temperature scale, not visible, starts from 0°K.

of the number of Bohr magnetons per molecule as

$$\begin{aligned}\mathcal{Y}_a&=B_S[(\tau/T)(\lambda\gamma_{aa}\mathcal{Y}_a-\mu\gamma_{ab}\mathcal{Y}_b)],\\ \mathcal{Y}_b&=B_S[(\tau/T)(-\lambda\gamma_{ab}\mathcal{Y}_a+\mu\gamma_{bb}\mathcal{Y}_b)],\end{aligned}\tag{4}$$

where $\tau=Ng^2\beta^2S^2/k$, with

$$\mathcal{Y}_a=M_a/\lambda Ng\beta S,\quad \mathcal{Y}_b=M_b/\mu Ng\beta S.$$

The net specific magnetization $\mathcal{Y}$ is given by

$$\mathcal{Y}=|\lambda\mathcal{Y}_a+\mu\mathcal{Y}_b|.\tag{5}$$

From this theory Néel has calculated $\mathcal{Y}$ as a function of the temperature and arranged the curves into various types according to their shapes. The classification is made in terms of the parameters α and β which are defined as follows:

$$\alpha=\gamma_{aa}/|\gamma_{ab}|\quad \beta=\gamma_{bb}/|\gamma_{ab}|.$$

The α's and β's give the strength and sign of the AA and BB interactions, respectively, in terms of the AB interaction.

In Fig. 5 we find certain types predicted by the above theory. In the case of the aluminates for t between 0 and 0.50, the curves follow the form we observed for ferromagnetic systems that are classified by Néel as Q curves. For $t=0$, we obtain a value of 2.20 Bohr magnetons per molecule for μ_0 in agreement with previous work.[13] When the amount of aluminum is increased by only a slight amount, to $t=0.63$, the magnetization increases with temperature like those curves predicted by Néel as his types M_1, M_2, or P. At $t=0.75$ the curve changes to nearly a straight line (Fig. 5) which holds approximately through to $t=1.00$. These curves are similar to those classified by Néel as type R which have been found to exist for zinc nickel ferrite and zinc manganese ferrite by Guillaud and Roux.[14] For greater amounts of aluminum, $t=1.25$, the curves return more nearly to the original form as for the nickel ferrite.

The increase in magnetization with increasing temperature found for the aluminates for $t=0.63$ is similar in shape to curves found by McGuire[15] for nickel chromite ($NiO\cdot Cr_2O_3$) and cobalt chromite ($CoO\cdot Cr_2O_3$).

In the present case, we have, instead of one type of magnetic ion, as developed by Néel, two of them which can occupy either or both the A or B sites; and, furthermore, one cannot assume that the g factor for a given magnetic ion will be the same in both the A and B sites. This imposes mathematical complexities, for Eqs. (2) through (5) would have to be modified accordingly before a detailed comparison with the theory could be accomplished. However, certain qualitative conclusions can be made.

Curves of the type R are represented on a β *vs* α plot by a restricted area whose position varies with the allowable values of λ and μ as shown by Fig. 9. We note that the area does not extend into positive values for β. This is the interpretation of the R-type curves for a system containing one kind of magnetic ion. We carry this interpretation to the present systems containing two kinds of magnetic ions on the assumption that they retain essentially the same features for the location of the R-type area on the β *vs* α plot (Fig. 9). This means that a negative BB interaction exists for those mixtures of the nickel ferrite-aluminate and nickel ferrite-gallate that give the R-type curves.

The R-type curves are constructed in Fig. 5 with a finite slope at absolute zero, although the lowest temperature at which these measurements were made was 75°K. Thermomagnetic measurements made on a zinc manganese ferrite (Ferroxcube III) by McGuire and Howard[16] at liquid helium temperature have shown a finite slope as the material is lowered in temperature to

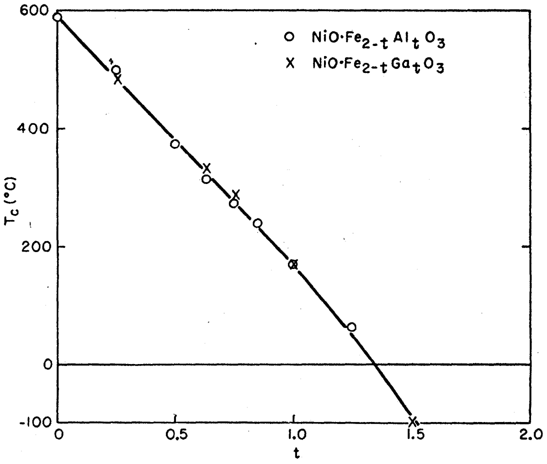

FIG. 8. Variation of Curie temperature (T_c) with composition for nickel ferrite-aluminates and nickel ferrite-gallates.

---

[13] See R. Pauthenet, Ann. phys. **7**, 710 (1952).

[14] C. Guillaud and M. Roux, Compt. rend. **229**, 1133 (1949); C. Guillaud, J. phys. et radium **12**, 239 (1951).

[15] T. R. McGuire (to be published).

[16] T. R. McGuire and L. N. Howard (to be published).

4°K. In view of the requirements of the third law of thermodynamics, we believe that in the region between 4°K and 0°K the curve for the zinc manganese ferrite bends over to zero slope at absolute zero. In the case of the present experiments, we are assuming that they also give a zero slope at absolute zero, with the departure from linearity occurring at a point near enough to 0°K as to give good values for the saturation magnetization by the methods used.

The way in which the saturation magnetization, extrapolated to absolute zero (μ_0), varies with composition, as shown by Fig. 6, indicates for the aluminates that the aluminum ions are going preferentially—but not entirely—into the B sites, thereby reducing the total magnetization as t varies from 0 to 0.63. For t from 0.75 to 2, μ_0 is plotted as negative, which gives a curve with no discontinuity in slope. At the crossover point we have found the situation where the magnetization of the ions in the A and B sites are equal in intensity but antiparallel. For greater amounts of aluminum, the magnetization from the A sites predominates; but as t increases further, the coupling weakens to that of a paramagnetic material at $t=2$. For the quenched samples, μ_0 decreases more slowly with increasing t in such a manner as to indicate that the B sites always predominate.

Gorter, Herbschleb, and Schulkes[17] have found data for the nickel ferrite-aluminate up to $t=1.0$ which is in agreement with our results shown in Fig. 6. The steepness of the curve as one approaches the crossover point depends upon the cooling rate—the less the rate, the steeper the curve until equilibrium is maintained throughout the cooling period. This fact was borne out by the work of Gorter, Herbschleb, and Schulkes[17] who were, we believe, the first to cool the material slowly enough to establish equilibrium conditions.

For the case of the gallates, starting from the nickel ferrite, the saturation moment increases indicating a preference of the gallium ions for the A sites, which results in a maximum at about the same place the aluminates pass through zero magnetization.

We find a Curie temperature of 590°C for the nickel ferrite (Fig. 8) without correcting for the effect of the applied field (4000 oersteds). This temperature is essentially in agreement with previous determinations.[18]

The Néel theory for the Curie temperature is expressed as follows:

$$T_c=\tfrac{1}{2}C\{\lambda\gamma_{aa}+\mu\gamma_{bb}+[(\lambda\gamma_{aa}-\mu\gamma_{bb})^2+4\lambda\mu\gamma_{ab}^2]^{\frac{1}{2}}\}, \quad (6)$$

where $C=Ng^2\beta^2S(S+1)/3k$. The way in which T_c varies with composition would be governed by changes in the coefficients λ and μ, after making certain modifications to allow for the fact that two separate magnetic ions are now involved as mentioned above. In view of this complexity, it is considered unlikely that a linear relationship would be observed. A slight departure from linearity for T_c has been found by Guillaud and Roux[14] for the zinc nickel ferrites as a function of the amount of zinc present.

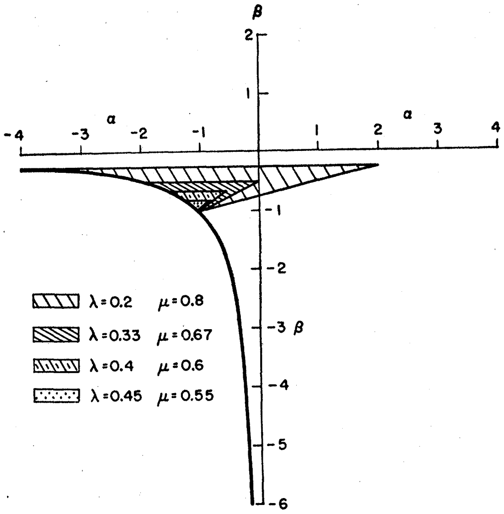

FIG. 9. Variation of Néel R-type area with magnetic ion distribution.

From the nature of our thermomagnetization curves, we observe that the exchange interactions, or the γ's, are certainly not identical for the aluminates and the gallates. It is, therefore, surprising that the Curie temperatures should be essentially the same, as a function of composition, for the aluminates and the gallates as shown in Fig. 8 in view of Eq. (6). Furthermore, one should expect a greater departure from linearity than we observe for the systems studied.

V. CONCLUSIONS

The substitution experiments replacing Fe^{3+} by Al^{3+} and Ga^{3+} furnish new significant facts concerning the magnetic behavior of ferrites as follows:

(a) Completely homogeneous nickel ferrite-aluminate and nickel ferrite-gallate systems can be prepared with a systematic linear variation in size of unit cell.

(b) The magnetic strength of the magnetic ions on the B and A sites can be varied relative to each other by the substitution of either Al^{3+} or Ga^{3+}, with a situation arising in the case of the aluminates where the magnetization on the B and A sites is equal and opposite.

(c) The case of the magnetization increasing with temperature, the Néel-type curves M_1, M_2, or P, is found for one of the nickel ferrite-aluminates ($t=0.63$).

(d) The R-type thermomagnetization curves predicted by Néel are found for certain nickel ferrite-aluminates and gallates.

(e) For the aluminates and gallates referred to in (d) above, it is concluded that the BB interaction is negative.

---

[17] Gorter, Herbschleb, and Schulkes (private communication).

[18] See Michel, Chaudron, and Bénard, J. phys. et radium 12, 189 (1951).

(f) The Curie temperatures are found to depend upon the number of nonmagnetic ions substituted independent of the type and to follow nearly a linear decrease with increasing concentration of Al^{3+} or Ga^{3+}.

VI. ACKNOWLEDGMENT

The writers are indebted to Dr. J. Samuel Smart for his valuable discussions in regard to the Néel theory as it applies to the problem considered in this paper; to Dr. T. R. McGuire for his suggestion that we use nickel ferrite for this substitution work and his help in the design and construction of the magnetic solenoids; to Dr. Francis Bitter for suggesting the type of solenoid used for producing the intense magnetic fields; to Mr. R. W. Hall who assisted in the early phases of the work; and to Dr. Roald K. Wangsness for the idea of the three-dimensional model for studying these magnetic systems.

PHYSICAL REVIEW VOLUME 92, NUMBER 5 DECEMBER 1, 1953

An Augmented Plane-Wave Method for the Periodic Potential Problem. II*

M. M. Saffren and J. C. Slater
Massachusetts Institute of Technology, Cambridge, Massachusetts

(Received August 31, 1953)

It is shown that the augmented plane-wave method recently proposed can be given an alternative interpretation which leads to a much simpler analytical formulation. We join a plane wave of energy E_0 outside the spherical atoms continuously, but with a derivative which is discontinuous, to spherical solutions of Schrödinger's equation inside the spherical atoms, corresponding to an energy E, to be determined. We compute the expectation value of the energy for this combined wave function, consisting of contributions from the plane-wave region, the spherical atoms, and also a surface contribution from the surface of the sphere, since the discontinuous derivative is equivalent to an infinite Laplacian which integrates to a finite contribution over the sphere. We now regard E as a parameter, and vary it to make the expectation value of energy stationary. The resulting wave function is proved to be identical with that set up in Part (I). Furthermore, the energy E inside the spheres proves to be identical with the expectation value of the energy, so that our functions are exact solutions of Schrödinger's equation inside the sphere, but not outside the sphere, since the energy of the plane wave E_0 is different from E. However this discrepancy is just canceled in the expectation value of energy by the surface integral. The resulting formulas for energy and wave function are much more convenient to use then those in Part (I).

THIS note forms an extension to the paper by one of the authors,[1] outlining a method for fitting approximate solutions of a spherical Schrödinger equation within the atoms of a crystal onto a plane wave in the region between the atoms. The reader is assumed to be familiar with this paper, which we shall describe as (I). In Eq. (9) of (I) we have set up the expansion coefficients of the assumed function within the spherical atoms, corresponding to energy values given by Eq. (8) of (I). Both these equations contain infinite sums which would be hard to evaluate in practice. By noting the resemblance of these sums to the expansions of Green's functions in terms of eigenfunctions of Schrödinger's equation, it occurred to one of us (MMS) that these sums in Eqs. (8) and (9) could be rewritten in a closed form. In this note we state the resulting equations, and the simple physical interpretation which can be given them.

Outside the atoms, in a region whose potential energy is taken to be zero, we have a plane wave of propagation vector k, energy E_0. Let us now set up a solution of Schrödinger's equation inside the ith spherical atom, with energy E [so far undetermined, though later to be identified with the E of (I)]. We build up this solution from solutions of the Schrödinger equation for each l value, for the assumed E; let such a solution, regular at the origin of the ith atom, be $u_{il}(E;r)$. We can superpose such functions, with appropriate coefficients, to set up a function which is continuous with the plane wave at the surface of the sphere; in general, however, the derivative will be discontinuous at the surface. We can now compute the expectation value of the energy for the wave function consisting of the plane wave of energy E_0 outside the sphere, and the spherical solution of energy E inside the sphere. There will be contributions to the integral of the Hamiltonian function consisting of E_0 times the integral of the square of the amplitude of the plane wave outside the sphere, and E times the integral of the square of the spherical solution inside the sphere. These are not the only contributions, however: on account of the discontinuity of derivative on the surface of the sphere, the Laplacian, or kinetic energy, is infinite there, and integrates to a finite contribution over the surface of the sphere.

We can now show that the augmented plane-wave function as set up in (I) is just such a function as we have described, in which further the expectation value of the energy is identical with the value E for which we

---

* Work assisted by the U. S. Office of Naval Research.

[1] J. C. Slater, Phys. Rev. 92, 603 (1953).

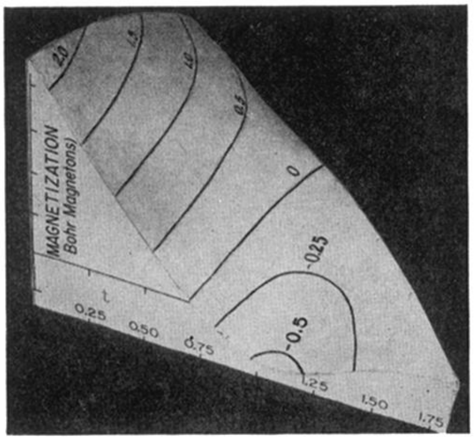

FIG. 7. Photograph of three dimensional model of the system nickel ferrite-aluminate. Temperature scale, not visible, starts from 0°K.